Inorganic Chemistry
Communication

*Inorg. Chem.* **2010**, *49*, 3679–3681 **3679**
DOI: 10.1021/ic902450c

# Construction of a $Ag_{12}$ High-Nuclearity Metallamacrocyclic 3D Framework

**Jiyong Hu,[†,‡] Jin'an Zhao,[†,‡] Qianqian Guo,[†] Hongwei Hou,[*,†] and Yaoting Fan[†]**

[†]*Department of Chemistry, Zhengzhou University, Henan 450052, People's Republic of China, and* [‡]*Department of Chemistry, Henan Univeristy of Urban Construction, Henan 467044, People's Republic of China*

Received December 10, 2009

An unprecedented high-nuclearity metallamacrocycle-based 3D silver framework with formula $\{[Ag_2(C_{25}H_{27}N_6O)_2](CH_3OH)(H_2O)_{0.17}\}_n$ (**1**), built on the basis of dodecanuclear silver building blocks, has been synthesized and characterized, and it shows strong phosphorescence emission at 10 K, which is a consequence of the presence of intersystem crossing from singlet to triplet caused by the heavy-atom effect of silver ions.

Up to now, a great many discrete metallamacrocycles with different sizes and shapes have been successfully achieved, in view of their potential applications in many areas such as molecular recognition, separation processes, and catalysis.[1] Also, the synthesis and characterization of high-dimensional polymers have been one intensely active research area because the polymers possess good thermal stability and can be extensively utilized in the fields of gas storage and separation, photonics, chemical sensing, etc.[2] In addition, the high-dimensional polymers on the basis of a polynuclear metallamacrocycle building block may show the potential for a more unique performance because of the combination of individual properties associated with a high-nuclearity macrocycle and polymer components.[3] Nevertheless, such complexes have been rarely reported.[3] Therefore, the design and construction of high-nuclearity macrocycle polymers should be given more attention.

To achieve these kinds of complexes, an organic ligand with specific functional groups and geometry is a major factor. The tetrazole ring possesses aromaticity and multiple coordinating modes, which can offer multiple coordinating sites for the bridging of closely situated metal ions, sustaining a diversity of polynuclear and even macrocyclic motifs.[4] Further, especially rich possibilities for high-nuclearity macrocyclic polymeric frameworks may be anticipated for the bifunctional ligand combining multidentate tetrazole and a monodentate coordinating site oriented in divergent fashion. Likewise, depending on the highly versatile and variable coordination number and geometry, the coordinative flexible silver(I) ion has also been of great interest for the construction of metal polymers.[5] Herein, a bifunctional tetrazole derivative, 2-butyl-3-[*p*-(0−1*H*-tetrazol-5-ylphenyl)benzyl]-1,3-diazospiro[4.4]non-1-en-4-ketone (Hbtpd), was employed to react with silver nitrate and, as a result, gave rise to an unprecedented dodecanuclear silver metallamacrocycle-based 3D framework $\{[Ag_2(btpd)_2](CH_3OH)(H_2O)_{0.17}\}_n$ (**1**). For macrocyclic metal polymers, no relevant studies and information concerning a high-nuclearity silver macrocycle as the building block have been present.[5b,6]

As can be seen from Figure S1 in the Supporting Information (SI), $btpd^-$ falls into two types of coordination. One acts as a bidentate ligand binding to two silver ions through two tetrazole nitrogen atoms; the other attaches to four silver ions by four nitrogen atoms, in which three nitrogen atoms are derives from the tetrazole group. The latter is different from most previously reported adducts, where the tetrazole usually serves as a mono- or bidentate ligand.[7] Both types of silver ions adopt trigonal coordination geometries. Each Ag1 is surrounded by three tetrazole nitrogen atoms, whereas each Ag2 completes its coordination sphere with two tetrazole nitrogen atoms as well as one diazospiro nitrogen atom. The combination of Ag1 and Ag2 via tetrazole bridges forms a dodecanuclear building block.

The dodecanuclear silver building block in **1** is an extraordinary structural feature (Scheme 1). For a metal−organic

*To whom correspondence should be addressed. Tel. and fax: +86-371-67761744. E-mail: houhongw@zzu.edu.cn.

(1) (a) Rauterkus, M. J.; Krebs, B. *Angew. Chem., Int. Ed.* **2004**, *43*, 1300–1303. (b) Ardizzoia, G. A.; Angaroni, M. A.; Monica, G. L.; Cariati, F.; Cenini, S.; Moret, M.; Masciocchi, N. *Inorg. Chem.* **1991**, *30*, 4347–4353. (c) Heath, S. L.; Sessoli, R.; Timco, G. A.; Winpenny, R. E. P. *Angew. Chem., Int. Ed.* **2004**, *43*, 6132–6135. (d) Cadiou, C.; Murrie, M.; Paulsen, C.; Winpenny, R. E. P. *Chem. Commun.* **2001**, 2666–2667. (e) Lehaire, M. L.; Scopelliti, R.; Piotrowski, H.; Severin, K. *Angew. Chem., Int. Ed.* **2002**, *41*, 1419–1422.

(2) (a) Kitagawa, S.; Kitaura, R.; Noro, S. *Angew. Chem., Int. Ed.* **2004**, *43*, 2334–2375. (b) Chen, B. L.; Ma, S. Q.; Hurtado, E. J.; Lobkovsky, E. B.; Zhou, H. C. *Inorg. Chem.* **2007**, *46*, 8490–8492. (c) Evans, O. R.; Lin, W. *Chem. Mater.* **2001**, *13*, 2705.

(3) (a) Moon, D.; Lah, M. S. *Inorg. Chem.* **2005**, *44*, 1934. (b) Moon, D.; Song, J.; Lah, M. S. *CrystEngComm* **2009**, *11*, 770–776.

(4) (a) Ferrer, S.; Lioret, F.; Bertomeu, I.; Alzuet, G.; Borrás, J.; Garcá-Grande, S.; Liu-González, M.; Haasnoot, J. G. *Inorg. Chem.* **2002**, *41*, 5821–5830. (b) Zhang, J. P.; Lin, Y. Y.; Huang, X. C.; Chen, X. M. *Dalton Trans.* **2005**, 3681–3685. (c) Dias, H. V. R.; Diyabalanage, H. V. K.; Gamage, C. S. P. *Chem. Commun.* **2005**, 1619–1621. (d) Li, H. X.; Wu, H. Z.; Zhang, W. H.; Ren, Z. G.; Zhang, Y.; Lang, J. P. *Chem. Commun.* **2007**, 5052–5054.

(5) (a) Blake, A. J.; Champness, N. R.; Cooke, P. A.; Nicolson, J. E. B. *Chem. Commun.* **2000**, 665–666. (b) Chen, C. L.; Kang, B. S.; Su, C. Y. *Aust. J. Chem.* **2006**, *59*, 3–18.

(6) Young, A. G.; Hanton, L. R. *Coord. Chem. Rev.* **2008**, *252*, 1346–1386.

(7) Wu, T.; Yi, B. H.; Li, D. *Inorg. Chem.* **2005**, *44*, 4130–4132.



Published on Web 03/15/2010

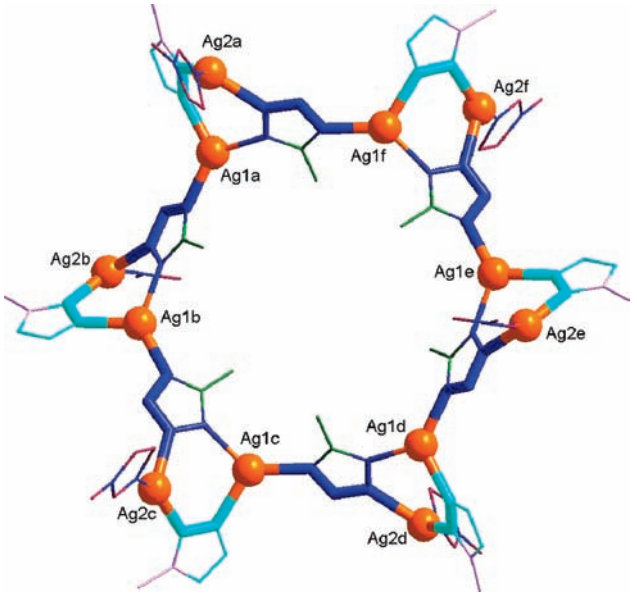


**Figure 1.** Arrangement of the 12 silver atoms of the metallacyclic unit in **1**. Parts of ligands are omitted for clarity.

**Scheme 1.** Building Block of **1** Formed via the Combination of Hbtpd and Silver(I)[a]

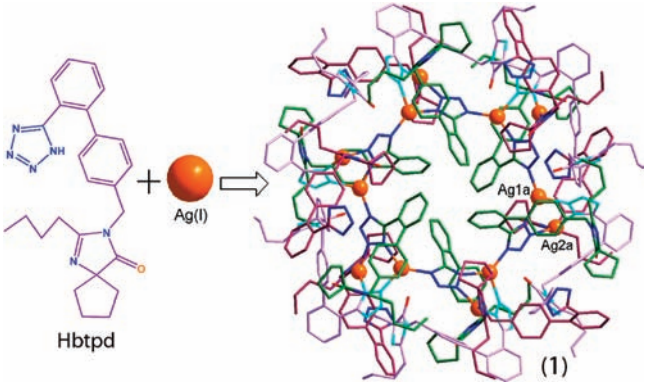


[a] Hydrogen atoms and solvent molecules are omitted for clarity.

macrocycle as the building block, Prakash and Lah reported a nanometer-sized hexanuclear or octanuclear manganese metallamacrocycle as the secondary building block to construct a two- or three-dimensional (2D or 3D) structure together with the ability to accommodate guest molecules; the Hong group also reported a three-dimemsional framework based on cadmium macrocycles and organic pillars.[8] In the present work, the arrangement of the silver ions in the building block resembles a crownlike metallamacrocycle (Figure 1). The six Ag1 ions lie in one plane (Ag1a−Ag1b−Ag1c−Ag1d−Ag1e−Ag1f); across the cavity, opposite silver ions are 13.1036 Å apart. The alternating dispositions of the remaining six Ag2 ions lie appreciably above (Ag2a−Ag2c−Ag2e) and below (Ag2b−Ag2d−Ag2f) the plane. The metal−metal separation is 3.7787(6) Å for Ag1 and Ag2. The cavity within the macrocycle is partially occupied by six phenyl groups, and every two facing phenyl

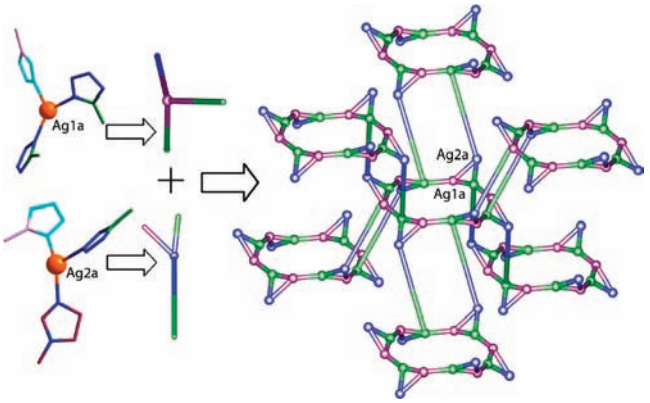


**Figure 2.** Simplified representation of the formation of one metallacyclic unit connecting to six adjoining ones along six directions. The bridging ligand is presented as a straight stick, and each tetrazolate group is shown as a sphere.

rings are parallel. The solvent-accessible volume was estimated by the *PLATON* program[9] to be 5% of the total crystal volume. The solvent molecules locate in the space between the macrocycles and around the diazospiro groups of bidentate btpd$^-$. As shown in Figure S2 in the SI, the weight loss of 3.51% from 30 to 170 °C corresponds to the release of solvent molecules (calcd 3.17%), and then it is stable up to 253 °C. Also, the spectrum of differential scanning calorimetry (DSC) exhibits an endothermic peak near 224 °C, which may indicate that **1** melts.

The dodecanuclear silver macrocycles are parallel and are arranged layer by layer. Each building block connects six adjoining ones via tetradentate btpd$^-$ along different orientations belonging to the adjacent layers to give rise to an unusual 3D coordination architecure (Figure 2). A better insight into the nature of the framework can be achieved by application of a topological approach. Taking Ag1, Ag2, and tetradentate btpd$^-$ as three-, three-, and four-connected nodes, respectively, the bidentate btpd$^-$ is simplified as a linear linker connecting Ag1 and Ag2 ions. The network can be described as a $(3\cdot6\cdot7)(3\cdot6\cdot7)(3\cdot6\cdot12^4)$ topology. After further analysis by the *OLEX* program, it is found that the vertex symbols of Ag1 as well as Ag2 are both $3\cdot6\cdot12\cdot3_3$, so topological analysis reveals that **1** is a binodal (3,4)-connected net with a symbol of $(3\cdot6\cdot7)_2(3\cdot6\cdot12^4)$ (Figure 3).

For the Raman spectrum of **1** (Figure S3 in the SI), the bands in the higher-frequency region (1000−1750 cm$^{-1}$) show the deformation and bend vibrational modes of benzene and tetrazole groups; the signals in the highest-frequency region (2800−3150 cm$^{-1}$) may be attributable to a CH stretching motion.[10] The photoluminescence of **1** and Hbtpd at room temperature (RT; Figure S4 in the SI) as well as 10 K (Figure S5 in the SI) was also inspected in the solid state. The powder X-ray diffraction (XRD) pattern of as-synthesized **1** is essentially identical with that simulated from the single-crystal X-ray data (Figure S6 in the SI). At RT, the emission spectrum of complex **1** results in a weak emission with $\lambda_{max}$ = 348 nm upon excitation at 285 nm, whereas Hbtpd emits strong fluorescence with excitation wavelength 280 nm. After cooling to 10 K, the emission spectrum of **1** excited at 288 nm consists of two emission bands: one weak

(8) (a) Prakash, M. J.; Lah, M. S. *Chem. Commun.* **2009**, 3326–3341. (b) Wang, R.; Hong, M.; Luo, J.; Cao, R.; Weng, J. *Chem. Commun.* **2003**, 1018–1019.

(9) Spek, A. L. *PLATON, A Multipurpose Crystallographic Tool*; Utrecht University: Utrecht, The Netherlands, 2003.

(10) Pergolese, B.; Bigotto, A. *J. Raman Spectrosc.* **2002**, *33*, 646–651.

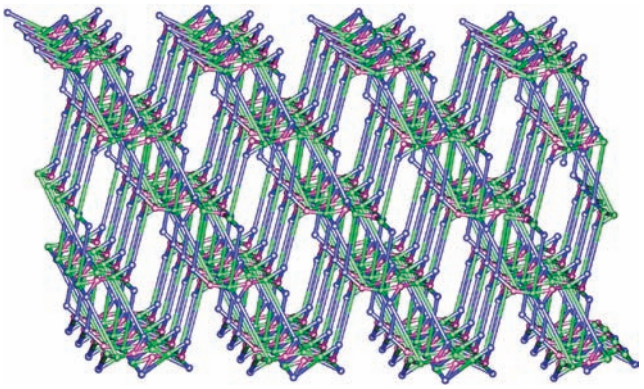

**Figure 3.** Schematic representation of the network of complex **1**.

fluorescence emission at 336 nm and one intense phosphorescence emission at 475 nm; for Hbtpd excited at 291 nm, the intense fluorescence emission at 336 nm and extremely weak phosphorescence emission at 475 nm are observed. As a heavy atom, the silver ion can effectively enhance the rate of intersystem crossing, which reduces fluorescence emission. Nevertheless, at RT, the nonradiative rate constant is very large, which is not conducive to observing phosphorescence.[11]

The fluorescence lifetimes for **1** at RT and 10 K yield $\tau$ = 0.3297 ± 0.01347 and 5.746 ± 0.410 ns, respectively, which are longer than the corresponding fluorescence lifetimes for Hbtpd, yielding $\tau$ = 0.2854 ± 0.01248 and 3.193 ± 0.0197 ns, respectively. This indicates that silver ions do negatively impact the fluorescence of Hbtpd because the increased lifetime can result in an effective decrease in the photostability. The phosphorescence lifetimes of **1** at RT and 10 K yield $\tau$ = 68.721 ± 1.062 $\mu$s and 80.08 ± 6.39 ms, respectively. For Hbtpd, the phosphorescence lifetime yields $\tau$ = 0.961 ± 0.131 s at 10 K, whereas no phosphorescence was observed at RT. At 10 K, the increased intensity of phosphorescence for **1**, in contrast to Hbtpd, is also in line with the decreased lifetimes and increased photostability.[12] Next, the emission lifetimes in the microsecond range or even longer, together with the large Stokes shift from the excitation maximum to the low-energy emission maximum of **1** and Hbtpd, are consistent with the fact that the low-energy emissions are associated with a spin-forbidden transition. Moreover, the emission bands of **1** and Hbtpd are similar in corresponding energy and band shape, so the emissions of **1** are tentatively assigned as metal-perturbed intraligand origins.[13]

In conclusion, a high-nuclearity macrocyclic 3D framework has been isolated. In comparison with Hbtpd, the quenching of the fluorescence of **1** is most likely a result of an enhanced intersystem crossing rate from the singlet state to the triplet excited state and a larger spin−orbit coupling constant caused by the silver heavy-atom effect.[14] It also contributes to the intensity increase of phosphorescence. Additionally, the inhibition of the nonradiative decay of the emitting triplet state and vibronic resolution upon cooling is favorable to the enhancement of phosphorescence as well.[15]

**Synthesis of** $\{[Ag_2(C_{25}H_{27}N_6O)_2](CH_3OH)(H_2O)_{0.17}\}_n$. A solution of $AgNO_3$ (0.0340 g, 0.2 mmol) in acetonitrile (2 mL), 2 drops of water, and an equivalent amount of Hbtpd in methanol (6 mL) were mixed, and colorless crystals were obtained upon slow evaporation of the solution in the dark at ambient temperature (yield: 56%, based on silver). Elem anal. Calcd for **1**: C, 55.39; H, 5.32; N, 15.20. Found: C, 54.99; H, 5.19; N, 15.28. IR (KBr): 3380 (m), 2959 (s), 2871 (m), 1716 (s), 1633 (s), 1562 (w), 1432 (m), 1402 (m), 1354 (s), 1223 (w), 1011 (m), 956 (w), 757 (s), 668 (w), 635 (w).

Empirical formula $\{[Ag_2(C_{25}H_{27}N_6O)_2](CH_3OH)(H_2O)_{0.17}\}_n$, formula weight 1105.84, crystal system trigonal, space group $R\bar{3}$, $a$ = 27.5892(10) Å, $b$ = 27.5892(10) Å, $c$ = 35.5762(17) Å, $\alpha$ = 90.00°, $\beta$ = 90.00°, $\gamma$ = 120.00°, $V$ = 23451.4(16) Å$^3$, and $Z$ = 18. $\mu$(Mo K$\alpha$) = 0.804 mm$^{-1}$, $\rho$ = 1.409 g cm$^{-3}$, reflection numbers collected = 67 509, unique reflections ($R_{int}$ = 0.0533) 10 239, GOF = 1.221. Data collection was performed on a Rigaku MM-OO7/Saturn 70, at $T$ = 113(2) K, using graphite-monochromated Mo K$\alpha$ radiation ($\omega$−2$\theta$ scans, $\lambda$ = 0.710 70 Å). Semiempirical absorption correction was applied for the complex. The structures were solved by direct methods and refined by full-matrix least squares. All calculations were done using the *SHELXTL-97* program system. Crystallographic agreement factors for the refinement are as follows: final $R$ indices [$I > 2\sigma(I)$], R1 = 0.0689, wR2 = 0.1643; $R$ indices (all data), R1 = 0.0716, wR2 = 0.1660.

**Acknowledgment.** This work was supported by the National Natural Science Foundation of China (Grant 20671082, 20971110 and J0830412), New Century Educational Talents Plan (Grant NCET-07-0765), and the Outstanding Talents Foundation by the Henan province.

**Supporting Information Available:** X-ray crystallographic file in CIF format, characterization, plots of TGA and DSC, $^1$H NMR spectrum, luminescence properties at RT and 10 K, and powder XRD. This material is available free of charge via the Internet at http://pubs.acs.org.

(11) Seward, C.; Chan, J.; Song, D.; Wang, S. *Inorg. Chem.* **2003**, *42*, 1112–1120.

(12) (a) Aslan, K.; Gryczynski, L.; Malicka, J.; Matveeva, E.; Lakowicz, J. R.; Geddes, C. D. *Curr. Opin. Biotechnol.* **2005**, *16*, 55–62. (b) Lakowicz, J. R. *Anal. Biochem.* **2001**, *298*, 1–24. (c) Yam, V. W. W.; Lo, K. K. W. *Chem. Soc. Rev.* **1999**, *28*, 323–334.

(13) Tao, C. H.; Yang, H.; Zhu, N.; Yam, V. W. W.; Xu, S. J. *Organometallics* **2008**, *27*, 5453–5458.

(14) (a) Wong, K. M. C.; Hong, L. L.; Lam, W. H.; Zhu, N.; Yam, V. W. W. *J. Am. Chem. Soc.* **2007**, *129*, 4350–4365. (b) Chao, H. Y.; Lu, W.; Li, Y.; Chan, M. C. W.; Che, C. M.; Cheung, K.-K.; Zhu, N. *J. Am. Chem. Soc.* **2002**, *124*, 14696–14706.

(15) Omary, M. A.; Patterson, H. H. *Inorg. Chem.* **1998**, *39*, 1060–1066.